Food and Chemical Toxicology 130 (2019) 317–325

Contents lists available at ScienceDirect

Food and Chemical Toxicology

journal homepage: www.elsevier.com/locate/foodchemtox

In silico and *in vivo* studies of *Astragalus glycyphylloides* saponin(s) with relevance to metabolic syndrome modulation

Merilin Al Sharif[a,*], Vessela Vitcheva[b], Rumyana Simeonova[b], Ilina Krasteva[c], Vasil Manov[d], Petko Alov[a], Georgi Popov[d], Aleksandar Shkondrov[c], Ilza Pajeva[a]

[a] Department of QSAR and Molecular Modelling, Institute of Biophysics and Biomedical Engineering, Bulgarian Academy of Sciences, Acad. G. Bonchev Str., bl. 105, 1113, Sofia, Bulgaria
[b] Department of Pharmacology, Pharmacotherapy and Toxicology, Faculty of Pharmacy, Medical University of Sofia, Dunav 2 Str., 1000, Sofia, Bulgaria
[c] Department of Pharmacognosy, Faculty of Pharmacy, Medical University of Sofia, Dunav 2 Str., 1000, Sofia, Bulgaria
[d] Department of Internal Non-communicable Diseases, Pathology and Pharmacology, Faculty of Veterinary Medicine, University of Forestry – Sofia, 10 Kliment Ochridsky Blvd., 1756, Sofia, Bulgaria

ARTICLE INFO

Keywords:
Metabolic syndrome
Saponins
Metabolites
PPARγ
Pharmacophore-based docking
Diabetic spontaneously hypertensive rats

ABSTRACT

Triterpenoids are well known modulators of metabolic syndrome. One of the suggested modes of action (MoAs) involves peroxisome proliferator-activated receptor gamma (PPARγ) binding.

In this study we aimed to: (i) evaluate *in silico* potential metabolites and PPARγ-mediated MoA of the sapogenin of the main saponin present in a purified saponins' mixture (PSM) from *Astragalus glycyphylloides*; (ii) estimate *in silico* and *in vivo* PSM's toxicity; and (iii) investigate *in vivo* antihyperglycaemic, hypolipidaemic, antioxidant and hepatoprotective effects of PSM.

Metabolites and toxicity were predicted using Meteor and Derek Nexus expert systems (Lhasa Limited) and PPARγ binding was investigated using the software MOE (CCG Inc.). PSM's acute oral toxicity was evaluated in mice and the pharmacological effects were assessed in streptozotocin-induced diabetic spontaneously hypertensive rats (SHRs). Liver histopathology was studied as well.

PPARγ weak partial agonism was predicted *in silico* for 24 probable/plausible Phase I metabolites which docking poses were clustered in 12 different binding modes with characteristic protein-ligand interactions. PSM's beneficial effects on the levels of blood glucose, triglycerides, and total cholesterol, on oxidative stress markers and liver histology in diabetic SHRs were comparable to those of the PPARγ ligand pioglitazone. PSM's safety profile was confirmed *in silico* and *in vivo*.

1. Introduction

The underlying mechanisms of metabolic syndrome pathogenesis include: insulin resistance, adipose tissue dysfunction, dyslipidaemia, glucose intolerance, chronic inflammation, oxidative stress and elevation of arterial blood pressure. As metabolic syndrome is associated with the increased risk for cardiovascular disease and type 2 diabetes, it has been generally emphasized as a serious health problem of high socioeconomic cost (Xu et al., 2018).

The interest toward implementation of naturally-derived compounds as functional foods and nutraceuticals in metabolic syndrome prevention and treatment has increased (Brown et al., 2015; Alkhatib et al., 2017; Santana-Gálvez et al., 2017). Metabolic syndrome modulation by pentacyclic triterpenes involves: reduction of insulin resistance and adipogenesis, increase in lipolysis, fatty acid oxidation and mitochondria biogenesis. The transcriptional regulators from the PPAR nuclear receptor family are among the mediators of these effects (Sharma et al., 2018). The oleanane-type sapogenin caulophyllogenin,

Abbreviations: BM, Binding mode; CAT, Catalase; DTNB, 2,2-Dinitro-5,5-dithiodibenzoic acid; GSH, Reduced glutathione; HB, Hydrogen bond; MDA, Malonedialdehyde; MoA, Mode of action; NADPH, Beta–nicotinamide adenine dinucleotide 2′-phosphate; PDB, Protein data bank; PLIFs, Protein-ligand interaction fingerprints; PPARγ, Peroxisome proliferator-activated receptor gamma; PSM, Purified saponins' mixture; ROS, Reactive oxygen species; SHR, Spontaneously hypertensive rats; SEM, Standard error of measurement; SOD, Superoxide dismutase; STZ, Streptozotocin; TBA, 2-Thiobarbituric acid; T2D, Type 2 diabetes

* Corresponding author.
E-mail addresses: merilin.al@biomed.bas.bg (M. Al Sharif), vesselavitcheva@yahoo.com (V. Vitcheva), rvitanska@gmail.com (R. Simeonova), krasteva.ilina@abv.bg (I. Krasteva), vmanov@ltu.bg (V. Manov), petko@biophys.bas.bg (P. Alov), gpopov@ltu.bg (G. Popov), a_shkondrov@abv.bg (A. Shkondrov), pajeva@biomed.bas.bg (I. Pajeva).

https://doi.org/10.1016/j.fct.2019.05.032
Received 8 April 2019; Received in revised form 15 May 2019; Accepted 19 May 2019
Available online 23 May 2019

with PPARγ relative maximal activation (E_{max}) of 9.4% (Montanari et al., 2016), has been co-crystallized in a complex with the receptor (Protein Data Bank ID 5F9B, ("PDB, www.rcsb.org,").

Our previous docking studies in the PPARγ pocket revealed potential weak partial agonistic binding modes of the oleanane-type sapogenin present in a purified saponins' mixture (PSM) from *Astragalus corniculatus*. This was supported by experimentally observed hypoglycaemic and antioxidant effects of PSM, comparable to those of pioglitazone (antidiabetic drug acting through PPARγ activation), in a model of spontaneously hypertensive rats (SHRs) with chemically induced type 2 diabetes (Al Sharif et al., 2018). In order to bring the *in silico* simulations of saponins closer to the real-life scenario, their *in vivo* metabolic activation by the gut microbiota enzymatic systems and the biotransformations in the liver have to be taken into account in the context of both potential toxic effects and therapeutic mechanism (Kim, 2018).

Astragalus glycyphylloides is a native for Bulgarian flora species. Previous phytochemical studies revealed that the plant contained flavonoids, i. e. quercetin, avicularin, hyperoside, isoquercitrin, kaempferol, isorhamnetin, isorhamnetin-3-glucoside and isorhamnetin-3-arabinoside (Kondeva-Burdina et al., 2013; Simeonova et al., 2013). Recently, a new saponin, 3-*O*-*β*-D-glucopyranosyl-28-*O*-[*β*-D-xylopyranosyl-(1 → 2)-*β*-D-glucopyranosyl] oleanolic acid was reported (Shkondrov et al., 2018). A total extract of the overground parts of the species showed both *in virto* and *in vivo* antioxidant and hepatoprotective effects, comparable to silymarin (Kondeva-Burdina et al., 2013; Simeonova et al., 2013) which gave the basis for this study. In the current study we aimed: (i) to evaluate *in silico* potential Phase I metabolites of the sapogenin of the main saponin present in PSM from *Astragalus glycyphylloides* and their PPARγ binding modes; (ii) to estimate *in silico* and *in vivo* PSM's toxicity; and (ii) to investigate *in vivo* the antidiabetic, hypolipidaemic, antioxidant and hepatoprotective effects of PSM on streptozotocin-induced diabetic SHRs.

2. Materials and methods

2.1. PSM preparation

Aerial parts of *A. glycyphylloides* DC. were collected in July 2016 from Rila Mountain, Bulgaria. The species was identified by Dr. D. Pavlova (Department of Botany, Faculty of Biology, Sofia University, voucher specimen № SO-093817).

The powdered plant material (400 g) was extracted and a purified saponins' mixture (PSM) was obtained as described before (Shkondrov et al., 2018). After HPLC analysis the saponin content was 60% (as oleanolic acid glycosides). One saponin was isolated from the PSM and identified by spectral data as 3-*O*-*β*-D-glucopyranosyl-28-*O*-[*β*-D-xylopyranosyl-(1 → 2)-*β*-D-glucopyranosyl] oleanolic acid (Fig. 1) (Shkondrov et al., 2018).

2.2. In silico studies

In silico studies were performed on the sapogenin of the saponins, present in PSM only (oleanolic acid), taking into account the bacterial-mediated and acid hydrolysis of the native sapogenin in the gastrointestinal tract (Chen et al., 2018).

2.2.1. Structures' preparation and molecular surface analysis

The structures of the sapogenin (oleanolic acid) and its predicted metabolites were built in MOE (Molecular Operating Environment (MOE), 2017) based on the isomeric SMILES code of oleanolic acid from the NIH PubChem system (CID: 10494 ("The PubChem Project,") as previously described (Al Sharif et al., 2018) and the 3D conformations were generated by "Flexible alignment" over caulophyllogenin's X-ray conformation (PDB ID: 5F9B) as a template. The correct protonation states of the structures at pH = 7.4 were assigned using the "Molecule wash" procedure in MOE.

The positioning of hydrogen atoms in the X-ray PPARγ protein structures and the assignment of their correct ionisation states, were performed using the "Protonate 3D" tool in MOE (Al Sharif et al., 2018).

2.2.2. Prediction of phase I metabolism

Meteor Nexus (v. 3.1.0) knowledge-based expert system (Knowledge Base: Meteor KB 2018 1.0.0) was employed for metabolite prediction (Langowski and Long, 2002; Marchant et al., 2008). In general, the reactive metabolites are produced by Phase I biotransformations (Njuguna et al., 2012), therefore a constraint was set for the Phase II metabolism predictions.

In order to predict Phase I metabolites in mammals the Absolute reasoning method was applied using minimal likelihood level = plausible ("Lhasa Limited,") and the default settings of maximal depth (number of metabolic steps) = 3 and maximal number of metabolites = 1000.

2.2.3. Toxicity prediction

For toxicity prediction Derek Nexus (v. 6.0.1) knowledge-based expert system (Knowledge Base: Derek KB 2018 1.1) (Marchant et al., 2008; "Lhasa Limited,") was employed. The minimal likelihood to consider a toxic outcome in the analysis was "plausible" (Al Sharif et al., 2017).

2.2.4. Molecular docking

Docking was performed as previously described (Al Sharif et al., 2018) using: PPARγ partial agonists (Table S1; Fig. S1A) for definition of the docking site in the protein structure (PDB ID 3D6D), a modified weak partial agonists' pharmacophore model (Fig. S1B) for placement and "Induced fit" option for the pose refinement (Molecular Operating Environment (MOE), 2017).

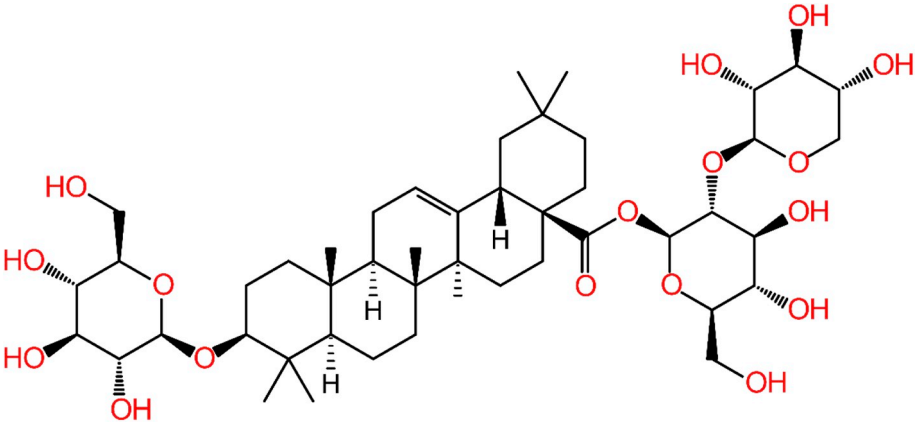

Fig. 1. Main saponin in *A. glycyphylloides*.

2.3. In vivo studies

2.3.1. Animals

Acute toxicity assessment of PSM involved 18 female mice. Experiments for estimation of the pharmacological profile of the PSM were performed on 24 adult male SHRs with initial body weight 300–350 g, obtained from Charles River Laboratories (Sulzfeld, Germany). The animals were housed in Plexiglas cages (3 per cage) at 20 ± 2 °C and under 12/12 h light/dark cycle. Food and water were provided *ad libitum*. All performed procedures were approved by the Bulgarian Food Safety Agency (BFSA) (permission № 168) and the principles stated in the European Convention for the Protection of Vertebrate Animals used for Experimental and other Scientific Purposes (ETS 123) (Council of Europe, 1991) were strictly followed. Blood pressure and body weight measurements were performed as previously described (Simeonova et al., 2016).

2.3.2. Chemicals

Streptozotocin, beta–nicotinamide adenine dinucleotide 2′-phosphate reduced tetrasodium salt (NADPH), trichloroacetic acid (TCA), 2-thiobarbituric acid (TBA), epinephrine, nicotinamide and pioglitazone were purchased from Sigma (Taufkirchen, Germany). 2,2-Dinitro-5,5-dithiodibenzoic acid (DTNB) was obtained from Merck (Darmstadt, Germany). All other reagents were of analytical grade.

2.3.3. Acute oral toxicity of PSM in mice

PSM was easily dissolved in physiological saline (0.9% NaCl) and administered by oral gavage at different doses at a dose volume of 1 mL/100 g bw.

The acute toxicity after oral (p.o.) administration of the tested PSM in 18 female mice was assessed using the simplified method of Lorke (1983). The experiment was performed in two phases. In the first phase nine animals, divided into three groups of three animals each were used. Each group of animals were administered different doses (10, 100 and 1000 mg/kg) of the PSM. Animals were inspected for signs of toxic effects and death, immediately after the oral administration of the PSM and every 2 h over the next 24 h.

In the second phase nine more mice were used, distributed into three groups of three animals each. The higher doses (1500, 3000 and 5000 mg/kg) of the PSM were administered orally and the animals were observed for 24 h.

The LD_{50} was calculated using the following equation:

$$LD_{50} = \sqrt{(D_0 \times D_{100})}$$

where D_0 is the highest dose that gave no mortality and D_{100} is the lowest dose that produced mortality.

2.3.4. Design of the experiment and type 2 diabetes induction

Twenty-four male SHRs were divided into four groups, each consisting of six animals (n = 6): control group (SHR C), diabetic SHRs (SHR DM), and diabetic SHRs, treated either with PSM (SHR DM + PSM) or the positive control pioglitazone (SHR DM + PG). The design of the experiment and the induction of type 2 diabetes mellitus in SHRs were performed as previously described (Fig. S2; (Al Sharif et al., 2018)). Rats with blood glucose levels of 9 mmol/l or more were considered to be diabetic and included in the study.

2.3.5. Blood biochemical parameters

Analysis of blood was performed at the beginning and at the end of the experiment (on the 1st and 22nd day). The blood was collected from the tail vein after a local anaesthesia and the levels of glucose, triglycerides and total cholesterol were measured using a Multiparameter diagnostic device “MultiCare-in” (Italy).

On the 22nd day after the blood pressure measurement and blood collection the animals were sacrificed by decapitation and livers were taken for determination of biomarkers of oxidative stress (malonedialdehyde, MDA and reduced glutathione, GSH) and activities of antioxidant enzymes (catalase, CAT and superoxide dismutase, SOD) as described in Al Sharif et al. (2018).

2.3.6. Histopathological evaluation

Livers were removed and fixed in 10% neutral buffered formalin. Thin sections (5 μm) were subsequently stained with haematoxylin/eosin for general histoarchitectonical features determination using light microscope Euromex BioBlue (Bancroft, 2008).

2.3.7. Statistical analysis

Statistical analysis was performed using ‘MEDCALC’, v. 12.3 (MedCalc Software, Belgium). Results were expressed as mean ± SEM for six rats in each group. The significance of the data was assessed using the non-parametric Mann–Whitney *U* test. Values of $p \leq 0.05$ were considered statistically significant.

3. Results and discussion

3.1. In silico studies

3.1.1. Prediction of phase I metabolism

An initial deglycosilation of saponins takes place *in vivo* (Yang et al., 2018). We selected the sapogenin (oleanolic acid) of the main saponin in PSM from *A. glycyphylloides* as a starting structure for Phase I metabolism prediction (Table 1).

Five types of biotransformations were predicted involving two enzymes. Alcohol dehydrogenase was predicted to catalyse the oxidation of secondary (alicyclic) alcohols, the reduction of alicyclic ketones, and the oxidation of primary alcohols, while CYP450 was predicted to catalyse the hydroxylation of methyl carbon adjacent to an aliphatic ring and the allylic hydroxylation of the structures.

Table 1
Predicted metabolites (M) with probable and *plausible* likelihood levels. The substituents at the predicted sites of metabolism (R1-R7) are highlighted in grey.

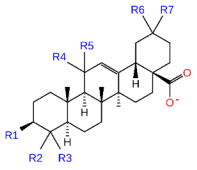

M	R1	R2	R3	R4	R5	R6	R7	PubChem CID
Oleanolic acid	**OH**	**CH_3**	**CH_3**	**H**	**H**	**CH_3**	**CH_3**	10494
M1	=O	CH_3	CH_3	H	H	CH_3	CH_3	12313704
M2.S	OH	CH_3	CH_2OH	H	H	CH_3	CH_3	12302577
M2.R	OH	CH_2OH	CH_3	H	H	CH_3	CH_3	73299
M3.S	OH	CH_3	CH_3	H	H	CH_3	CH_2OH	12314864
M3.R	OH	CH_3	CH_3	H	H	CH_2OH	CH_3	21594136
M6.S	OH	CH_3	CH_3	OH	H	CH_3	CH_3	
M6.R	OH	CH_3	CH_3	H	OH	CH_3	CH_3	73353448
M10.S	=O	CH_2OH	CH_3	H	H	CH_3	CH_3	
M10.R	=O	CH_3	CH_2OH	H	H	CH_3	CH_3	12310388
M11.S	=O	CH_3	CH_3	H	H	CH_3	CH_2OH	
M11.R	=O	CH_3	CH_3	H	H	CH_2OH	CH_3	10790565
M13.S	=O	CH_3	CH_3	OH	H	CH_3	CH_3	
M13.R	=O	CH_3	CH_3	H	OH	CH_3	CH_3	15864059
M25.S	OH	COO-	CH_3	H	H	CH_3	CH_3	15560324
M25.R	OH	CH_3	COO-	H	H	CH_3	CH_3	
M33.S	OH	CH_3	CH_3	H	H	CH_3	COO-	12315597
M33.R	OH	CH_3	CH_3	H	H	COO-	CH_3	21594175
M35	OH	CH_3	CH_3	=O	-	CH_3	CH_3	
M48.S	=O	COO-	CH_3	H	H	CH_3	CH_3	
M48.R	=O	CH_3	COO-	H	H	CH_3	CH_3	
M64.S	=O	CH_3	CH_3	H	H	CH_3	COO-	
M64.R	=O	CH_3	CH_3	H	H	COO-	CH_3	101951534
M74	=O	CH_3	CH_3	=O	-	CH_3	CH_3	

The substituents of 24 metabolites, 17 with probable likelihood of occurrence and 7 with plausible likelihood (including the duplicate of the starting structure), are listed in Table 1 and the detailed metabolic tree is presented in Fig. S3.

The metabolites include unique structures and stereoisomeric couples. The central ring of the oleanolic acid (R4/R5) was metabolised only in 3 out of 20 predicted reactions generating M6, M13, M35, and M74, while the most frequently predicted sites of metabolism were at the peripheral rings of the structure (R1, R2/R3 and R6/R7). Fourteen of the predicted oleanolic acid metabolites (Table 1) were identified in the NIH PubChem system ("The PubChem Project,"). Among them are the following sapogenins: oleanonic acid (M1), 4-epihederagenin (M2.S), hederagenin (M2.R), queretaroic acid (M3.S), mesembryanthemoidigenic acid (M3.R), hederagonic acid (M10.R), gypsogenic acid (M25.S), spergulagenic acid (M33.S), and serratagenic acid (M33.R). In the literature a weak partial agonism (E_{max} = 20%) toward PPARγ has been reported for the oleanonic acid (Petersen et al., 2011). Moreover, this sapogenin has been known for its anti-hyperglycaemic effect (Kawabata et al., 2017). We also found relevant experimental data for hederagenin (compound 5) and its glycosides (compounds 1, 3, 6, and 7) which have been shown to possess PPARγ transactivation activity (Quang et al., 2011). Furthermore, inhibitory effects on plasma triglyceride elevation have been shown for the principle saponin constituents from *Sapindus rarak* DC., having hederagenin as an aglycon (Asao et al., 2009). The reported biotransformations could also have impact on the binding of the compounds to the receptor. To investigate them, the specific protein-ligand interaction fingerprints (PLIFs) and binding modes were studied by molecular docking.

3.1.2. Prediction of toxicity

Although oleanolic acid is generally considered as safe (Liu, 1995), metabolic activation may generate an array of derivatives and their safety profiles have to be considered as well. In our previous study on naturally-derived modulators of non-alcoholic fatty liver disease we have shown Derek Nexus predictions of toxic alerts that appeared after Phase I biotransformations and were missing in the starting structures (Al Sharif et al., 2017). Therefore, in the current study we performed Derek Nexus predictions of all studied metabolites of the oleanolic acid. The 24 metabolites were predicted to be inactive in the bacterial *in vitro* (Ames) mutagenicity test. Furthermore, no toxic effects with a likelihood of plausible or higher were reported for the 60 additional endpoints covered by the program (Table S2). Further, *in vivo* experiments were performed to confirm the good safety profile of the PSM (see Section 3.2.1. Acute oral toxicity of PSM in mice.

3.1.3. Molecular docking

The docking studies were performed in the sub-pocket of the receptor typically occupied by agonists with relative efficacy below 35% (Fig. S1A, Table S1 in the Supplementary data) and a pharmacophore model for a weak partial agonistic type of activity was applied in the initial pose generation step (Fig. S1B). Thus, all poses that successfully passed the simulation were suggested to induce a moderate activation of PPARγ. In the comparative analysis of the docking poses, 12 different binding modes (BMs) were outlined (Table S3) with a characteristic occupancy of the receptor pocket (Fig. S4) and/or distinct PLIFs (Table S4). Overall, Phase I biotransformations resulted in metabolites with increased electronegative areas on their van der Waals interaction molecular surfaces which suggests influence on their capacity to interact with key amino acids in the receptor pocket in a multi-conformational manner (Fig. S5).

Five binding modes (BM 1 – BM 5) have higher frequencies of occurrence (8–24 metabolites, Fig. S6A) and three of these reproduced excellently (BM 3) or resembled (BMs 1 and 2) the caulophyllogenin's X-ray pose (Fig. S4B).

Five other binding modes (BM 8 – BM 12) are characteristic for a single metabolite and thus are termed singular (Table S3). These are predicted for metabolites M64.S (1), M33.R (1), M13.R (2) and M74 (1). Metabolites M13.R and M64.S have the broadest spectrum of binding modes – 7 and 6, correspondingly (Table S3). M64.S occupies the pocket with four common BMs (listed in the top 5 most frequent ones), and with only one alternative BM (ratio 4 : 1), M13.R binds the receptor with three common and four alternative BMs (ratio 3 : 4). The alternative BMs of M13.R are shared by M6.R and M74 (BMs 6 and 7) and M35 (BM 6) and these metabolites are related to biotransformations at the central ring (R4/R5) of the oleanolic acid (Table 1). Additionally, M13.R displays two singular BMs – 10 and 11 (Table S3). Obviously, the combination of carbonyl group at R1 and hydroxyl group at R5 (Table 1) increases the variability of the ligand-receptor interactions of M13.R as compared to the rest of the metabolites (M6.S, M6.R, M35, and M74) from that branch of the tree (Fig. S3).

On the other hand, M64.S is representative for the larger subset of metabolites, metabolised at the two peripheral rings of the triterpenoid skeleton, which explains the appearance of the structure among the most frequently predicted BMs. However, M64.S displays one more binding mode (BM 8, Fig. S4) which is singular and relates to a unique HB acceptor interaction with Ile 326 (H5) (Table S3). The presence of

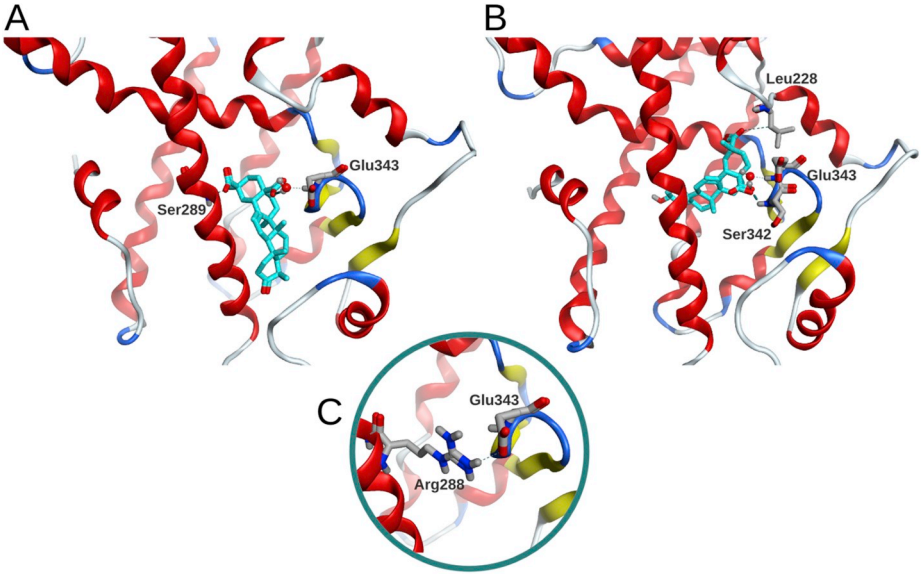

Fig. 2. Protein-ligand interactions of dicarboxylic metabolites: A. M64.S, displaying BM 5, performs HB interaction with Ser289 (H3), in addition to the commonly predicted water-mediated contact with Glu343 (β-sheet), allowing the bulky part of the structure to fit in the Ω-loop at the bottom, B. M33.R with a singular BM 9, forms contacts with Leu228 (H1–H2 loop), Ser342 (β-sheet), and Glu343 (β-sheet), leaving the hydrophobic part of the structure in the sub-pocket outlined by H3, H5 and H7, C. Stabilising intra-protein interaction between Arg288 (H3) and Glu343 (β-sheet), triggered by the two metabolites. Rendering: ligands (cyan carbon atoms) and amino acids (element type colouring) are displayed in a stick mode, water molecules (element type colouring) – in a ball and stick mode. (For interpretation of the colours in this figure, the reader is referred to the Web version of this article.)

two carboxylic substituents at the small distance of four C-atoms is characteristic only for the stereoisomeric couples of M64 and M33. Such a topological feature points to the engagement of both carboxylic groups in specific PLIFs (Table S4; Fig. 2 A, B). The protein-anchoring networks, mediated by M64.S and M33.R, are further stabilised by a intra-protein interaction of Glu343 (β-sheet) with Arg288 (H3) (Fig. 2C), the latter usually being engaged with HB acceptor and/or ionic interactions with the carboxyl group of the triterpenoid scaffold.

The metabolite with the lowest number of different binding modes (only 2), and thus the most stable positioning within the pocket, was the R form of M64. This result poses the question about the role of triterpenoid's stereoisomery for the diversity in the modes of PPARγ pocket occupancy.

Generally, two major groups of BMs for the stereo-couples are observed (Table S3). The first one is a conservative receptor binding (BMs 1 and 2) that is unaffected by stereoisomery at the sites of metabolism of the triterpenoid scaffold. The second one is a variable, stereo-specific receptor binding (BMs 4 and 5) which is predicted only for one of the stereoisomers in the couple and thus quantitatively contributes in a unique manner to the overall frequency of the particular BM. Comparative analysis of the predicted BMs and sites of metabolism reveals a high number of non-shared BMs for the stereoisomeric couples of M6, M13, M64, and M33 (shaded, Table S3). These metabolites possess carboxyl substituent at positions R6/R7 (M64, M33) or hydroxyl substituent at positions R4/R5 (M6, M13), which are distinctive and rarely occurring substructures within the predicted series of metabolites (Table 1). This might be the reason for their diverse behaviour in the receptor pocket, as compared to the rest of the metabolites having stereocentres at their sites of metabolism.

Although the BM clusters possess characteristic PLIFs (Table S4), contacts involving Arg288 (H3) and Ser342 (β-sheet), which are typical for the weak partial agonists (Al Sharif et al., 2018) and water-mediated interaction with Glu343 (β-sheet) are the most frequently predicted ones (Fig. 3). The BM 3, holding the highly scored poses, is associated with all aforementioned contacts plus two additional stabilising HB acceptor interactions with His323 (H5, water-mediated, Fig. 3C) or even more often, Lys367 (H7, Fig. 3D). The latter is an amino acid residue which, due to its flexible and thus highly adaptive side chain, participates in a stabilising intra-protein network that involves Met364 and Phe363 (turn in H7) and His449 (H11).

In the PLIFs of the singular binding modes, Arg288 and Ser342 can: (i) be the only amino acid residues performing specific interactions that stabilise the ligand in the pocket, (ii) interact with the ligand in combination with other amino acids like Cys285 (H3) or Leu228 (H1–H2 loop), or (iii) be substituted by alternative pose anchoring points, related to hydrogen bonding with Leu330 or Ile326 from H5.

The molecular docking scores are an estimation of the free energy of binding of the predicted protein-ligand complexes. Although there is no clear correlation between the receptor binding affinity and the docking scores, the latter could give us a clue about the relevance of the predictions. The average docking scores of all predicted poses for given metabolite were analysed together with the best and worst docking scores (Table S5). These average values range between −13.9 and −12.8 kcal/mol, the latter being predicted for the poses of the oleanolic acid (Table S5). The metabolites with average scoring below the lowest quartile of distribution (from −13.9 to −13.4 kcal/mol) are related to modifications at the following peripheral sites of metabolism: R1-R3 (M2.R, M10.R, M25.S, M48.S) or R6-R7 (M3.R). Among these metabolites M10.R and M25.S were predicted to occupy the receptor pocket with the best scored poses of −16.4 and −16.1 kcal/mol, respectively. When performing redocking of the X-ray pose of caulophyllogenin, applying the same docking simulation settings as in the screening protocol of the oleanolic acid metabolites, all poses reproduced the X-ray binding mode with a scoring range between −15.0 and −12.7 kcal/mol (average −13.9 kcal/mol). These data indicate that the predicted protein-ligand complexes have binding energies comparable to those of the X-ray complex of caulophyllogenin with PPARγ and the studied metabolites could be pharmacologically active.

Our findings for potential PPARγ binding by the sapogenin (oleanolic acid) and its metabolites, are in accordance with previous experimental studies on PPARγ modulation by triterpenoids. A series of oleanolic acid derivatives found in the stem bark of *Kalopanax pictus* (Araliaceae) have been reported to activate PPARγ in a HepG2 cell line. In particular, compound 9 (possessing an oleanolic acid sapogenin) has been reported to transactivate PPARγ with EC_{50} = 17.1 ± 0.9 μM (Quang et al., 2011).

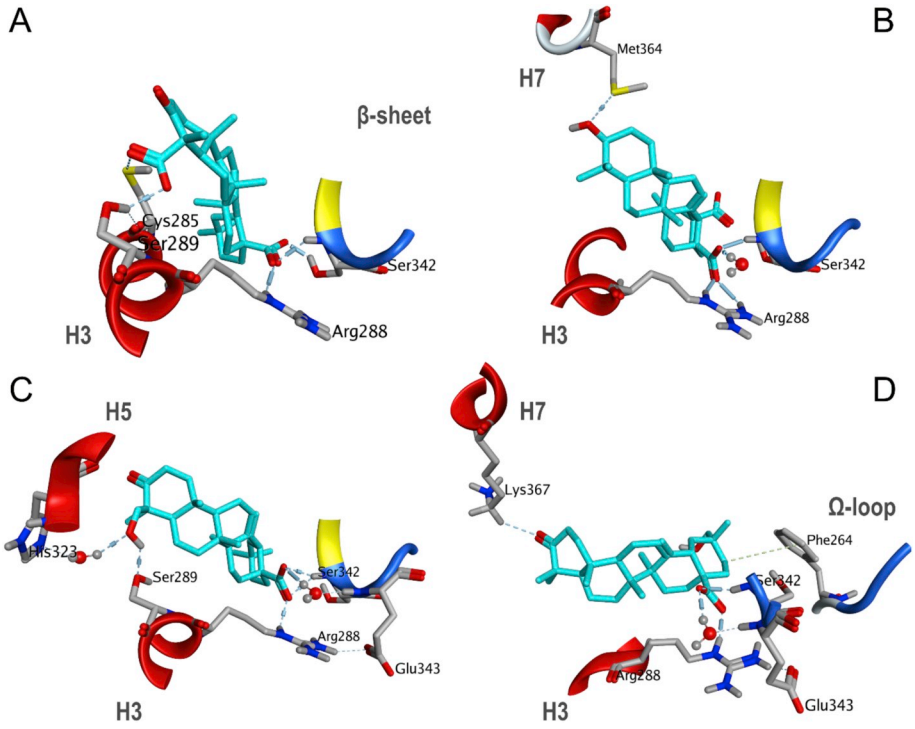

Fig. 3. Representative protein-ligand interactions of the three most frequent binding modes (Table S3) among the predicted metabolites (Table 1). A. BM 1, M48.S; B. BM2, M33.S; C. BM 3, M10.S, D. BM 3, M11.R. Rendering: ligands (cyan carbon atoms) and amino acids (element type colouring) are displayed in a stick mode, water molecules (element type colouring) – in a ball and stick mode. (For interpretation of the colours in this figure, the reader is referred to the Web version of this article.)

Table 2
Acute p.o. toxicity of PSM in female mice.

Compound	1st phase		2nd phase	
	Doses mg/kg p.o.	Mortality	Doses mg/kg p.o.	Mortality
PSM	10	0/3	1500	0/3
	100	0/3	3000	1/3
	1000	0/3	5000	3/3

3.2. In vivo studies

3.2.1. Acute oral toxicity of PSM in mice

In the first phase the animals were treated with 10, 100, and 1000 mg/kg of the tested PSM and all of them survived the acute oral treatment without apparent symptoms. In the second phase, the animals were treated with the higher doses: 1500, 3000, and 5000 mg/kg. The results on the acute oral toxicity of the PSM are summarised in Table 2. The acute toxicity test showed that the PSM is nontoxic (LD_{50} = 2121 mg/kg p.o. in mice).

Based on the results obtained, LD_{50} p.o. for PSM is above 2000 mg/kg for mice, so it could be classified as less dangerous or non-toxic when administered orally to mice.

For *in vivo* study 1/20 from LD_{50} (≈100 mg/kg) was used.

3.2.2. Pharmacological studies

Spontaneously hypertensive rats are the most widely studied animal model of essential hypertension in which increased blood pressure has been reported together with other risk factors for cardiovascular disease, including insulin resistance and dyslipidaemia (Pravenec et al., 2004). In the *in vivo* studies we focused on evaluation of the antidiabetic, antioxidant and antihypertensive potential of PSM obtained from *A. glycyphylloides*, using a model of streptozotocin-induced type 2 diabetes in SHRs.

3.2.2.1. Changes in body weight and systolic blood pressure. All animals survived till the end of the experiment. No clinical signs of toxicity were observed. The changes in the mean body weight of all groups are shown in Table 3. For the study period control SHR group gained weight by 24 g. SHR DM rats lost 28 g of body weight by the end of the study (22 days after treatment). The diabetic SHRs treated with PSM and PG did not change significantly their weight during the experiment.

STZ itself decreased blood pressure in SHRs by 14% ($p < 0.05$), compared to non-treated SHRs, which is in a good agreement with the investigation of Erejuwa et al. (2011) and is probably due to decreased body weight, compared to SHR controls. PSM treatment did not change significantly the blood pressure in diabetic SHRs compared to SHR DM group. Pioglitazone treatment additionally reduced blood pressure with 13%, compared to SHR DM, which supports the findings of Majithiya et al. (2005). Antihypertensive effect of oleanolic acid has been recently reported in a rat model of pre-diabetes (Gamede et al., 2019).

Table 4
Blood level of glucose, triglycerides and total cholesterol.

Group	Blood glucose level (mmol/L)	Triglycerides (mmol/L)	Total cholesterol (mmol/L)
SHR C	4.90 ± 0.48	0.48 ± 0.03	1.25 ± 0.09
SHR DM	9.92 ± 0.81*	0.77 ± 0.07*	2.34 ± 0.20*
SHR DM + PSM	7.34 ± 0.51*+	0.61 ± 0.05*+	1.97 ± 0.10*+
SHR DM + PG	6.24 ± 0.75*+	0.52 ± 0.09+	1.69 ± 0.19*+

Data are expressed as mean ± SEM of six rats (n = 6).
*$p < 0.05$ vs SHR control group.
+$p < 0.05$ vs diabetic SHR group.

3.2.2.2. Changes in blood glucose level, triglycerides and total cholesterol. Hyperlipidaemia often coexists with hyperglycaemia and is characterized by increased levels of cholesterol and triglycerides and changes in lipoproteins (Andallu et al., 2009). The blood glucose levels were significantly ($p < 0.05$) elevated in the STZ-induced diabetic SHR (by 102.4%), compared to their matched controls (Table 4).

The serum levels of triglycerides and total cholesterol were also increased by 60% ($p < 0.05$), and by 84.2% ($p < 0.05$) respectively, compared to control SHRs. PSM decreased in statistically significant manner blood glucose level by 26%, triglycerides by 21% and total cholesterol by 16% compared to diabetic SHRs. The effects of PSM on blood biochemical parameters were comparable with the effects of the positive control pioglitazone.

Saponins are reported to possess a number of pharmacological properties, among which antioxidant, antihyperlipidaemic and antidiabetic effects (Lee et al., 2000). Furthermore, an oleanolic acid treatment of diet-induced pre-diabetic rat model has been shown to result in a significant decrease in the levels of triglycerides and in amelioration of dyslipidaemia (Gamede et al., 2019). In a study on the beneficial effects of nano-formulation of oleanolic acid in the treatment of insulin-resistance and metabolic disorders in high fat and fructose diet-fed rats, a reduction of the increased serum triglycerides and cholesterol has been shown (Wang et al., 2018).

Kuroda et al. (2012) have reported that oleanolic acid, although having a moderate transactivation activity, contributed to the potent PPARγ ligand-binding activity of the clove (*Syzygium aromaticum*) EtOH extract, and the hypoglycaemic effects of this extract on genetically diabetic KK-A^y has been partially attributed to PPARγ modulation. Recently, α-amyrin-induced upregulation of PPARγ has been proposed as one of the molecular mechanisms explaining the antidiabetic effect of this oleanane-type sapogenin (Giacoman-Martínez et al., 2019).

3.2.2.3. Markers of oxidative stress and antioxidant enzymes. STZ-induced diabetes resulted in oxidative stress, discerned by markedly increased MDA formation by 31% ($p < 0.05$), GSH depletion by 32% ($p < 0.05$) and decreased activities of CAT by 25% ($p < 0.05$) and SOD by 42% ($p < 0.05$) (Fig. 4).

The beneficial effect of PSM treatment in diabetic animals was evidenced by significant increase ($p < 0.05$) in GSH levels by 66%,

Table 3
Changes in body weight and systolic blood pressure.

Animal group	Systolic blood pressure (mm Hg)	Change %		Mean body weight (g)		
		vs SHR C	vs SHR DM	Initial	Final	Change
SHR C	226 ± 11.4			336 ± 8.2	360 ± 4.8	+24
SHR DM	194 ± 8.3	−14*		340 ± 6.3	312 ± 6.2	−28
SHR DM + PSM	201 ± 13.0	−11	+4	338 ± 9.7	342 ± 4.6	+4
SHR DM + PG	169 ± 6.6	−25*	−13+	326 ± 9.2	332 ± 6.8	+6

Data are expressed as mean ± SEM of six rats (n = 6).
*$p < 0.05$ vs SHR control group.
+$p < 0.05$ vs diabetic SHR group.

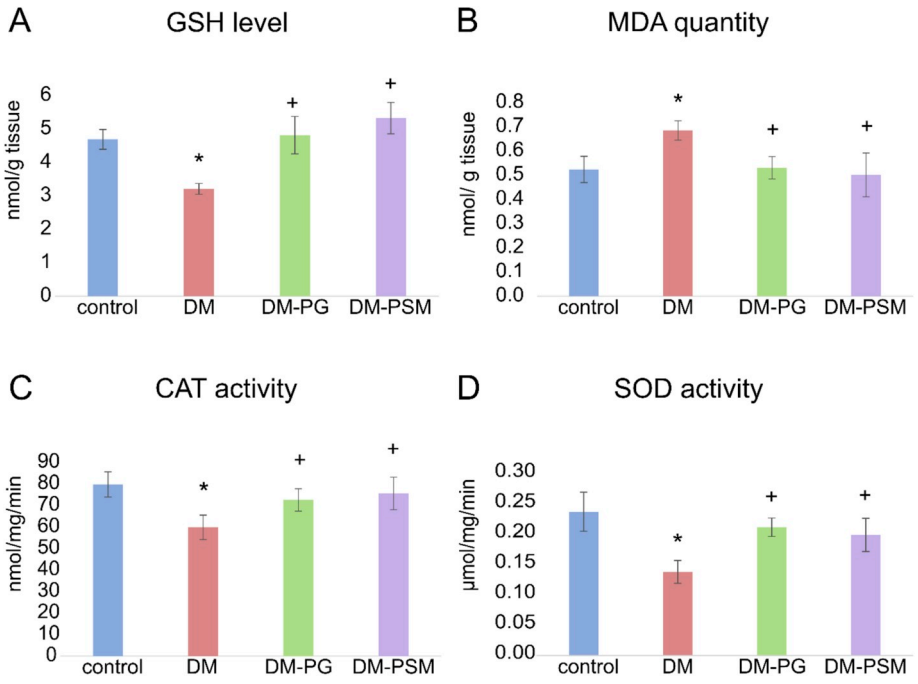

Fig. 4. Antioxidant effects of PSM and pioglitazone in control and diabetic SHRs: A. Levels of GSH, B. Quantity of MDA, C. CAT activity, D. SOD activity. Data are expressed as mean ± SEM of six rats (n = 6); $^{*}p < 0.05$ vs SHR control group; $^{+}p < 0.05$ vs diabetic SHR group.

while MDA production was decreased ($p < 0.05$) by 27% (Fig. 4 A, B). The effect of NA/STZ on the antioxidant enzymes activity of CAT and SOD was prevented by PSM treatment. CAT activity was 26% higher ($p < 0.05$) and SOD – 44% higher ($p < 0.05$) in PSM-treated group compared to SHR DM group (Fig. 4 C, D).

Diabetes and hypertension are two of the most frequent non-communicable diseases of our modern society, which often occur together and oxidative stress is regarded as one of the main pathophysiological mechanisms in both disorders (Cheung and Li, 2012). Our results are in accordance with the reported by Chan et al. (2018) and Chen et al. (2014) antioxidant effects of saponins on the SOD activity and MDA level.

The induced hyperglycaemia in the present experiment was accompanied by body weight reduction, increased MDA production and decreased antioxidant defence (GSH, CAT and SOD) (Fig. 4) which support the findings of Haluzík and Nedvídková (2000), who have shown that the cytotoxic effect of STZ can be partially mediated by release of nitric oxide and ROS. Regarding this mode of STZ action, antihyperglycaemic and hypotensive effects are suggested for the bio-antioxidants in patients with diabetes and hypertension co-morbidity.

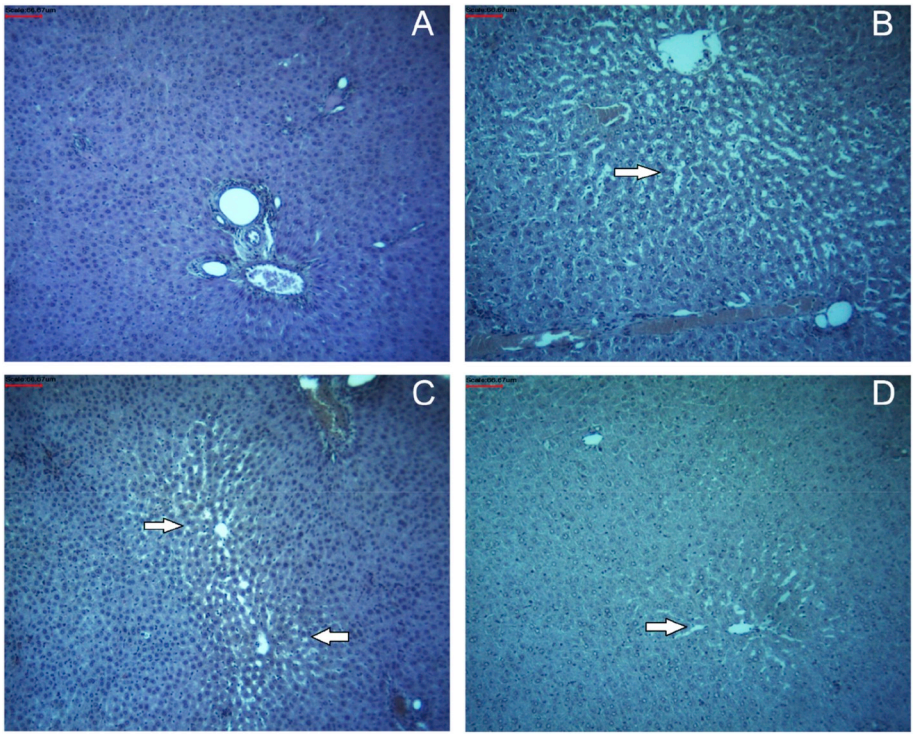

Fig. 5. Pathohistological analysis of livers (haematoxylin and eosin, line bar length – 66.67 µm) of SHRs: A. Liver of a rat from control group. Normal histological structure; B. Liver of a rat treated with NA/STZ. Hepatocytes with unclear borders and microgranular cytoplasm; C. Liver of a diabetic rat, treated with PSM; D Liver of a diabetic rat, treated with pioglitazone.

Recently, administration of oleanolic acid has been shown to ameliorate oxidative stress in pre-diabetes rat model (Gamede et al., 2019). Treatment of high fat and fructose diet-fed rats with nano-oleanolic acid, has been reported to result in an efficacious mitigation of the increased MDA levels and the SOD and CAT activities in blood samples (Wang et al., 2018).

In our study the antioxidant effect of PSM was comparable with the effect of the positive control pioglitazone. El-Mas et al. (2011) have shown that pioglitazone could abrogate the oxidative (aortic SOD and MDA) and dyslipidaemic effects of cyclosporine-induced abnormalities in hypertension. An increasing body of evidence is pointing to PPARγ-mediated oxidative stress alleviation by regulation of CAT and manganese SOD expression (Polvani et al., 2012).

3.2.3. Histopathological studies

The control group showed normal histological and cellular architecture with distinct hepatocytes, spaces of Disse, central veins and tracts (Fig. 5A). In the livers of rats treated with NA/STZ the hepatic cells were disarranged (swollen appearance, cloudy cytoplasm and microgranulations). The swollen cells affected space of Disse and the lumen of the sinusoidal capillaries was narrowed (Fig. 5B). The liver sections of the diabetic SHRs, treated with PSM, showed swollen hepatocytes with unclear, microgranular cytoplasm, located in the centrilobular zones (Fig. 5C). Livers from animals of the positive control group revealed similar histological parameters as well. In the livers of diabetic SHRs, treated with pioglitazone, in the centrilobular areas only single swollen cells were observed (Fig. 5D). These findings suggest that PSM had a protective effect on the liver at histological level commensurable to pioglitazone. The observed hepatoprotective effects are in accordance with similar studies on triterpenoids like akebia saponin D (Gong et al., 2016) and glycyrrhizic acid (Sil et al., 2015).

4. Conclusion

On the basis of molecular docking simulations, a PPARγ weak partial agonism was suggested for the sapogenin of the main saponin in PSM from *Astragalus glycyphylloides* and for its metabolites predicted *in silico*. Clustering of docking poses according to the binding mode and the protein-ligand interaction fingerprints underlined the role of the predicted sites of metabolism for the diversity of the PPARγ binding. *In silico* toxicity prediction resulted in a good safety profile for all docked structures and the PSM's safety was confirmed by *in vivo* acute oral toxicity assessment in mice.

The developed novel protocol for *in silico* prediction of possibly co-existing metabolites, their potential toxic effects and therapeutic MoAs could further be broadened to aid the prioritisation of naturally-derived molecular scaffolds bearing optimal potential to serve as drug-discovery leads, nutraceuticals or as components of new functional foods.

The *in vivo* antidiabetic, antioxidant and antihypertensive potential of PSM, was investigated using a model of NA/STZ-induced type 2 diabetes in spontaneously hypertensive rats. It could be concluded that administration of PSM to diabetic rats improved their glycaemic and liver biochemical and antioxidant status. The histological examination proved that the PSM had hepatoprotective effect which was less pronounced compared to pioglitazone, in rats with artificially induced type 2 diabetes mellitus.

Conflicts of interest

The authors declare no conflict of interests.

Declaration of interests

The authors declare that they have no known competing financial interests or personal relationships that could have appeared to influence the work reported in this paper.

Acknowledgments

Studies on prediction of Phase I metabolism and toxicity were supported by the Bulgarian Ministry of Education and Science under the National Research Programme "Healthy Foods for a Strong Bio-Economy and Quality of Life" approved by DCM # 577/17.08.2018; the molecular docking studies, part of the *in vivo* experiments and the pathohistological analysis were supported by the National Science Fund of Bulgaria (grant DM 01/1/2016).

Transparency document

Transparency document related to this article can be found online at https://doi.org/10.1016/j.fct.2019.05.032

Appendix A. Supplementary data

Supplementary data to this article can be found online at https://doi.org/10.1016/j.fct.2019.05.032.

References

Al Sharif, M., Alov, P., Diukendjieva, A., Vitcheva, V., Simeonova, R., Krasteva, I., Shkondrov, A., Tsakovska, I., Pajeva, I., 2018. Molecular determinants of PPARγ partial agonism and related in silico/in vivo studies of natural saponins as potential type 2 diabetes modulators. Food Chem. Toxicol. 112, 47–59. https://doi.org/10.1016/j.fct.2017.12.009.

Al Sharif, M., Alov, P., Vitcheva, V., Diukendjieva, A., Mori, M., Botta, B., Tsakovska, I., Pajeva, I., 2017. Natural modulators of nonalcoholic fatty liver disease: mode of action analysis and in silico ADME-Tox prediction. Toxicol. Appl. Pharmacol. 337, 45–66. https://doi.org/10.1016/j.taap.2017.10.013.

Alkhatib, A., Tsang, C., Tiss, A., Bahorun, T., Arefanian, H., Barake, R., Khadir, A., Tuomilehto, J., 2017. Functional foods and lifestyle approaches for diabetes prevention and management. Nutrients 9, 1310. https://doi.org/10.3390/nu9121310.

Andallu, B., Vinay Kumar, A., Varadacharyulu, Nc., 2009. Lipid abnormalities in streptozotocin-diabetes: amelioration by Morus indica L. cv Suguna leaves. Int. J. Diabetes Dev. Ctries. 29, 123. https://doi.org/10.4103/0973-3930.54289.

Asao, Y., Morikawa, T., Xie, Y., Okamoto, M., Hamao, M., Matsuda, H., Muraoka, O., Yuan, D., Yoshikawa, M., 2009. Structures of acetylated oleanane-type triterpene saponins, rarasaponins IV, V, and VI, and anti-hyperlipidemic constituents from the pericarps of Sapindus rarak. Chem. Pharm. Bull. (Tokyo) 57, 198–203. https://doi.org/10.1248/cpb.57.198.

Bancroft, J.D., 2008. Theory and Practice of Histological Techniques. Elsevier Health Sciences.

Brown, L., Poudyal, H., Panchal, S.K., 2015. Functional foods as potential therapeutic options for metabolic syndrome: foods as the treatment of obesity. Obes. Rev. 16, 914–941. https://doi.org/10.1111/obr.12313.

Chan, K.W., Ismail, M., Mohd Esa, N., Mohamed Alitheen, N.B., Imam, M.U., Ooi, D.J., Khong, N.M.H., 2018. Defatted Kenaf (*Hibiscus cannabinus* L.) seed meal and its phenolic-saponin-rich extract protect hypercholesterolemic rats against oxidative stress and systemic inflammation via transcriptional modulation of hepatic antioxidant genes. 2018. Oxidative Med. Cell. Longev. 1–11. https://doi.org/10.1155/2018/6742571.

Chen, M.-Y., Shao, L., Zhang, W., Wang, C.-Z., Zhou, H.-H., Huang, W.-H., Yuan, C.-S., 2018. Metabolic analysis of Panax notoginseng saponins with gut microbiota-mediated biotransformation by HPLC-DAD-Q-TOF-MS/MS. J. Pharm. Biomed. Anal. 150, 199–207. https://doi.org/10.1016/j.jpba.2017.12.011.

Chen, Y., Miao, Y., Huang, L., Li, J., Sun, H., Zhao, Y., Yang, J., Zhou, W., 2014. Antioxidant activities of saponins extracted from Radix Trichosanthis: an in vivo and in vitro evaluation. BMC Complement Altern. Med. 14. https://doi.org/10.1186/1472-6882-14-86.

Cheung, B.M.Y., Li, C., 2012. Diabetes and hypertension: is there a common metabolic pathway? Curr. Atheroscler. Rep. 14, 160–166. https://doi.org/10.1007/s11883-012-0227-2.

Council of Europe, 1991. Council of Europe [WWW Document]. Council of Europe. European Convention for the Protection of Vertebrate Animals Used for Experimental and Other Scientific Purposes. CETS No. 123, 1991. http://www.coe.int/en/web/conventions/full-list/-/conventions/treaty/123 (accessed 6.27.18).

El-Mas, M.M., El-Gowelli, H.M., Abd-Elrahman, K.S., Saad, E.I., Abdel-Galil, A.-G.A., Abdel-Rahman, A.A., 2011. Pioglitazone abrogates cyclosporine-evoked hypertension via rectifying abnormalities in vascular endothelial function. Biochem. Pharmacol. 81, 526–533. https://doi.org/10.1016/j.bcp.2010.11.013.

Erejuwa, O.O., Sulaiman, S.A., Wahab, M.S.A., Sirajudeen, K.N.S., Salleh, M.S.M., Gurtu, S., 2011. Differential responses to blood pressure and oxidative stress in streptozotocin-induced diabetic wistar-kyoto rats and spontaneously hypertensive rats: effects of antioxidant (honey) treatment. Int. J. Mol. Sci. 12, 1888–1907. https://doi.org/10.3390/ijms12031888.

Gamede, M., Mabuza, L., Ngubane, P., Khathi, A., 2019. Plant-derived oleanolic acid (OA) ameliorates risk factors of cardiovascular diseases in a diet-induced pre-diabetic rat

model: effects on selected cardiovascular risk factors. Molecules 24 pii: E340. https://doi.org/10.3390/molecules24020340.
Giacoman-Martínez, A., Alarcón-Aguilar, F.J., Zamilpa, A., Hidalgo-Figueroa, S., Navarrete-Vázquez, G., García-Macedo, R., Román-Ramos, R., Almanza-Pérez, J.C., 2019. Triterpenoids from Hibiscus sabdariffa L. With PPARδ/γ dual agonist action: in vivo, in vitro and in silico studies. Planta Med. 85, 412–423. https://doi.org/10.1055/a-0824-1316.
Gong, L. -l., Li, G. -r., Zhang, W., Liu, H., Lv, Y. -l., Han, F. -f., Wan, Z. -r., Shi, M. -b., Liu, L. -h., 2016. Akebia saponin D decreases hepatic steatosis through autophagy modulation. J. Pharmacol. Exp. Ther. 359, 392–400. https://doi.org/10.1124/jpet.116.236562.
Haluzík, M., Nedvídková, J., 2000. The role of nitric oxide in the development of streptozotocin-induced diabetes mellitus: experimental and clinical implications. Physiol. Res. 49 (Suppl. 1), S37–S42.
Kawabata, K., Kitamura, K., Irie, K., Naruse, S., Matsuura, T., Uemae, T., Taira, S., Ohigashi, H., Murakami, S., Takahashi, M., Kaido, Y., Kawakami, B., 2017. Triterpenoids isolated from Ziziphus jujuba enhance glucose uptake activity in skeletal muscle cells. J. Nutr. Sci. Vitaminol. 63, 193–199. https://doi.org/10.3177/jnsv.63.193.
Kim, D.-H., 2018. Gut microbiota-mediated pharmacokinetics of ginseng saponins. J. Ginseng Res. 42, 255–263. https://doi.org/10.1016/j.jgr.2017.04.011.
Kondeva-Burdina, M., Simeonova, R., Krasteva, I., Benbassat, N., 2013. Protective effects of extract from Astragalus glycyphylloides on carbon tetrachloride-induced toxicity in isolated rat hepatocytes. Biotechnol. Biotechnol. Equip. 27, 3866–3869.
Kuroda, M., Mimaki, Y., Ohtomo, T., Yamada, J., Nishiyama, T., Mae, T., Kishida, H., Kawada, T., 2012. Hypoglycemic effects of clove (Syzygium aromaticum flower buds) on genetically diabetic KK-Ay mice and identification of the active ingredients. J. Nat. Med. 66, 394–399. https://doi.org/10.1007/s11418-011-0593-z.
Langowski, J., Long, A., 2002. Computer systems for the prediction of xenobiotic metabolism. Computational Methods for the Prediction of ADME and Toxicity. Adv. Drug Deliv. Rev. 54, 407–415. https://doi.org/10.1016/S0169-409X(02)00011-X.
Lee, K.T., Sohn, I.C., Kim, D.H., Choi, J.W., Kwon, S.H., Park, H.J., 2000. Hypoglycemic and hypolipidemic effects of tectorigenin and kaikasaponin III in the streptozotocin-lnduced diabetic rat and their antioxidant activity in vitro. Arch Pharm. Res. (Seoul) 23, 461–466.
Lhasa Limited [WWW Document]. https://www.lhasalimited.org/ (accessed 6.27.18).
Liu, J., 1995. Pharmacology of oleanolic acid and ursolic acid. J. Ethnopharmacol. 49, 57–68. https://doi.org/10.1016/0378-8741(95)90032-2.
Lorke, D., 1983. A new approach to practical acute toxicity testing. Arch. Toxicol. 54 (4), 275–287.
Majithiya, J., Paramar, A., Balaraman, R., 2005. Pioglitazone, a PPARγ agonist, restores endothelial function in aorta of streptozotocin-induced diabetic rats. Cardiovasc. Res. 66, 150–161. https://doi.org/10.1016/j.cardiores.2004.12.025.
Marchant, C.A., Briggs, K.A., Long, A., 2008. In silico tools for sharing data and knowledge on toxicity and metabolism: Derek for windows, meteor, and vitic. Toxicol. Mech. Methods 18, 177–187. https://doi.org/10.1080/15376510701857320.
Molecular Operating Environment (MOE), 2017. Chemical Computing Group Inc., 1010 Sherbooke St. West, Suite #910, Montreal, QC, Canada, H3A 2R7.
Montanari, R., Capelli, D., Tava, A., Galli, A., Laghezza, A., Tortorella, P., Loiodice, F., Pochetti, G., 2016. Screening of saponins and sapogenins from Medicago species as potential PPARγ agonists and X-ray structure of the complex PPARγ/caulophyllogenin. Sci. Rep. 6. https://doi.org/10.1038/srep27658.
Njuguna, N.M., Masimirembwa, C., Chibale, K., 2012. Identification and characterization of reactive metabolites in natural products-driven drug discovery. J. Nat. Prod. 75, 507–513. https://doi.org/10.1021/np200786j.
PDB, www.rcsb.org [WWW Document]. http://www.rcsb.org/pdb/home/home.do (accessed 6.27.18).
Petersen, R.K., Christensen, K.B., Assimopoulou, A.N., Fretté, X., Papageorgiou, V.P., Kristiansen, K., Kouskoumvekaki, I., 2011. Pharmacophore-driven identification of PPARã agonists from natural sources. J. Comput. Aided Mol. Des. 25, 107–116. https://doi.org/10.1007/s10822-010-9398-5.
Polvani, S., Tarocchi, M., Galli, A., 2012. PPAR and oxidative stress: con%28%29 catenating NRF2 and FOXO. PPAR Res. 2012 1–15. https://doi.org/10.1155/2012/641087.
Pravenec, M., Zídek, V., Landa, V., Šimáková, M., Mlejnek, P., Kazdová, L., Bílá, V., 2004. Genetic Analysis of "Metabolic Syndrome" in the Spontaneously Hypertensive Rat, vol. 53. pp. 8.
Quang, T.H., Ngan, N.T.T., Minh, C.V., Kiem, P.V., Thao, N.P., Tai, B.H., Nhiem, N.X., Song, S.B., Kim, Y.H., 2011. Effect of triterpenes and triterpene saponins from the stem bark of Kalopanax pictus on the transactivational activities of three PPAR subtypes. Carbohydr. Res. 346, 2567–2575. https://doi.org/10.1016/j.carres.2011.08.029.
Santana-Gálvez, J., Cisneros-Zevallos, L., Jacobo-Velázquez, D., 2017. Chlorogenic acid: recent advances on its dual role as a food additive and a nutraceutical against metabolic syndrome. Molecules 22, 358. https://doi.org/10.3390/molecules22030358.
Sharma, H., Kumar, P., Deshmukh, R.R., Bishayee, A., Kumar, S., 2018. Pentacyclic triterpenes: new tools to fight metabolic syndrome. Phytomedicine 50, 166–177. https://doi.org/10.1016/j.phymed.2018.09.011.
Shkondrov, A., Krasteva, I., Bucar, F., Kunert, O., Kondeva-Burdina, M., Ionkova, I., 2018. Flavonoids and saponins from two Bulgarian Astragalus species and their neuroprotective activity. Phytochem. Lett. 26, 44–49. https://doi.org/10.1016/j.phytol.2018.05.015.
Sil, R., Ray, D., Chakraborti, A.S., 2015. Glycyrrhizin ameliorates metabolic syndrome-induced liver damage in experimental rat model. Mol. Cell. Biochem. 409, 177–189. https://doi.org/10.1007/s11010-015-2523-y.
Simeonova, R., Krasteva, I., Kondeva-Burdina, M., Benbassat, N., 2013. Effects of extract from Astragalus glycyphylloides on carbon tetrachloride-induced hepatotoxicity in Wistar rats. Int. J. Pharma Bio Sci. 4, 179–186.
Simeonova, R., Vitcheva, V., Krasteva, I., Zdraveva, P., Konstantinov, S., Ionkova, I., 2016. Antidiabetic and antioxidant effects of saponarin from Gypsophila trichotoma on streptozotocin-induced diabetic normotensive and hypertensive rats. Phytomedicine 23, 483–490. https://doi.org/10.1016/j.phymed.2016.02.024.
The PubChem Project [WWW Document]. https://pubchem.ncbi.nlm.nih.gov/ (accessed 6.27.18).
Wang, S., Du, L.B., Jin, L., Wang, Z., Peng, J., Liao, N., Zhao, Y.Y., Zhang, J.L., Pauluhn, J., Hai, C.X., Wang, X., Li, W.L., 2018. Nano-oleanolic acid alleviates metabolic dysfunctions in rats with high fat and fructose diet. Biomed. Pharmacother. 108, 1181–1187. https://doi.org/10.1016/j.biopha.2018.09.150.
Xu, H., Li, X., Adams, H., Kubena, K., Guo, S., 2018. Etiology of metabolic syndrome and dietary intervention. Int. J. Mol. Sci. 20, 128. https://doi.org/10.3390/ijms20010128.
Yang, B., Li, H., Ruan, Q., Tong, Y., Liu, Z., Xuan, S., Jin, J., Zhao, Z., 2018. Rapid profiling and pharmacokinetic studies of multiple potential bioactive triterpenoids in rat plasma using UPLC/Q-TOF-MS/MS after oral administration of Ilicis Rotundae Cortex extract. Fitoterapia 129, 210–219. https://doi.org/10.1016/j.fitote.2018.07.005.